AGU PUBLICATIONS

Geophysical Research Letters

RESEARCH LETTER
10.1002/2015GL063096

**Key Points:**
- The ratio TEC/Nmax of a planetary ionosphere represents the slab thickness
- Slab thickness relates to the neutral atmosphere's scale height and temperature
- Mars' ionosphere has a nighttime slab thickness of 25 km that doubles in daytime

**Correspondence to:**
C. Narvaez,
cnarvaez@bu.edu

**Citation:**
Mendillo, M., C. Narvaez, G. Lawler, W. Kofman, J. Mouginot, D. Morgan, and D. Gurnett (2015), The equivalent slab thickness of Mars' ionosphere: Implications for thermospheric temperature, *Geophys. Res. Lett.*, *42*, 3560–3568, doi:10.1002/2015GL063096.

Received 13 JAN 2015
Accepted 6 APR 2015
Accepted article online 10 APR 2015
Published online 5 MAY 2015



# The equivalent slab thickness of Mars' ionosphere: Implications for thermospheric temperature

**M. Mendillo[1], C. Narvaez[1], G. Lawler[1], W. Kofman[2,3], J. Mouginot[4], D. Morgan[5], and D. Gurnett[5]**

[1]Center for Space Physics, Boston University, Boston, Massachusetts, USA, [2]Institut de Planetologie et d'Astrophysique, Grenoble, France, [3]Space Research Centre of the Polish Academy of Sciences, Warsaw, Poland, [4]Department of Earth System Science, University of California, Irvine, California, USA, [5]Department of Physics and Astronomy, University of Iowa, Iowa City, Iowa, USA

**Abstract** The total electron content (TEC) of a planetary ionosphere is dominated by plasma near and above the height of maximum electron density ($N_{max}$). The ratio TEC/$N_{max}$ represents the thickness ($\tau$) of a TEC slab of uniform density ($N_{max}$). For a photochemical ionosphere, $\tau$ relates to the scale height ($H = kT/mg$) of the ionized neutral gas as $\tau \sim 4 \times H$. Derived temperatures refer to ~160 km in thermosphere height—below the asymptotic temperature of the exosphere. The MARSIS instrument on Mars Express has produced data sets of TEC and $N_{max}$. We used them to form $\tau$ patterns versus solar zenith angle and solar cycle phase. For daytime (SZA $< 90°$) conditions, $<\tau>_{day} \sim 50$ km, decreasing rapidly for solar zenith angle (SZA) $> 90°$ to $<\tau>_{night} \sim 25$ km. These correspond to $T_n$ values of 250°K and 125°K. Using Mars Global Surveyor data, $\tau$ patterns show a mild dependence upon the solar EUV flux proxy $F_{10.7}$, with $\Delta T_n(°K) \sim 0.3°$ per unit change in $F_{10.7}$ at Mars.

## 1. Introduction

The ionosphere of a planet or moon is best described by its profile of electron density versus height, $N_e(h)$. This is precisely the observational product of a radio occultation experiment—with profiles available for Venus, Mars, the giant planets, and some of their moons. Mars is second only to Earth for the number of ionospheric profiles available for study. As shown in Table 1 in *Mendillo et al.* [2003], there were a total of 433 profiles obtained from several satellites spanning the years 1965–1978, and then 5600 profiles from the Mars Global Surveyor (MGS) satellite during discrete observing periods between December 1998 and June 2005 [*Hinson et al.*, 1999]. The currently operational Mars Express (MEX) satellite has a radio occultation experiment [*Pätzold et al.*, 2005] that has produced approximately 700 profiles from April 2004 to the present.

MEX has an additional capability to make ionospheric measurements at Mars. The *Mars Advanced RADAR for Subsurface and Ionospheric Studies* (MARSIS) can retrieve ionospheric parameters in two ways: (a) the "Active Ionospheric Sounding (AIS)" mode functions as an *ionosonde* of the topside ionosphere [*Gurnett et al.*, 2005]. High-frequency (HF) transmissions are reflected at the various plasma frequencies of electron densities from the altitude of maximum density ($N_{max}$) to the satellite height ($N_{sat}$); (b) the "Subsurface (SS) mode" [*Picardi et al.*, 2005] uses HF transmission to reach the surface (and below). The returned radar signal is distorted by its two-way transmission through the ionosphere. This "degradation" can be carefully removed to yield the total electron content, $TEC = \int N_e(h) dh$ [*Safaeinili et al.*, 2007; *Mouginot et al.*, 2008]. The MARSIS experiments that yield $N_{max}$ and TEC can be conducted at all latitudes and local times accessible from the MEX orbit, and thus offer the first comprehensive way to explore the Martian ionosphere beyond the near-terminator conditions inherent in the radio occultation technique [*Fox and Yeager*, 2006]. Here we conduct the first joint study of $N_{max}$ and TEC available from MARSIS, and show that their ratio can be used to enhance our current understanding of the Martian ionosphere and thermosphere.

## 2. Background

### 2.1. A Semiempirical Model of Maximum Electron Density

The MARSIS/AIS observations yielded approximately 112,000 values of $N_{max}$ spanning the period 15 August 2005 to 8 June 2012. These data were used in conjunction with the photochemical equilibrium (PCE)

condition to arrive at the Mars Initial Reference Ionosphere model described in *Mendillo et al*. [2013a]. Their functional form relating $N_{max}$ to the solar radio flux ($F_{10.7}$), used as a proxy for solar ultraviolet radiation, and the solar zenith angle (SZA) to portray diurnal patterns, is given by

$$N_{max}\left(e^{-}/m^{3}\right) = 2.3 \times 10^{10} \times \sqrt{\cos(\mathrm{SZA}) \times \mathrm{RF}} \quad (1)$$

where RF is the effective radio flux proxy at 1.524 AU given by

$$\mathrm{RF} = \left[F_{10.7(\mathrm{day})} + F_{10.7(81-\mathrm{day})}\right] / 2 \quad (2)$$

Further details of the model and its validation are given in *Mendillo et al*. [2013a].

### 2.2. A Semiempirical Model of Total Electron Content

The initial MARSIS/SS observations of TEC included approximately 1.4 million values distributed over the planet from 19 June 2005 to 30 September 2007. These data were initially analyzed by *Safaeinili et al*. [2007], *Mouginot et al*. [2008], and *Lillis et al*. [2010] to show that they followed the basic equations of PCE theory—subsequently confirmed by *Cartacci et al*. [2013] using a larger amount of data. Our initial study of TEC at Mars used the MARSIS archive of high-quality flag-1 data (~1.2 million values) to document ionospheric variability patterns versus location on Mars under both daytime and nighttime conditions [*Mendillo et al*., 2013b]. Using the subset of these data that pertain to daytime conditions (SZA ≤ 90°) and the identical analysis used for $N_{max}$ that led to equation (1), the following functional relation was found

$$\mathrm{TEC}\left(e^{-}/m^{2}\right) = 1.2 \times 10^{15} \times \sqrt{\cos(\mathrm{SZA}) \times \mathrm{RF}} \quad (3)$$

with RF as specified in (2).

### 2.3. The Equivalent Slab Thickness of an Ionosphere

For Earth, the ionospheric parameters most observed from vast networks of radio receivers are $N_{max}$ (from ground-based ionosondes) and TEC (from GPS satellites). As expected from the fact that the integral of a $N_e(h)$ profile is dominated by plasma close to the height of maximum density, these two parameters are highly correlated (~90%), as shown in *Fox et al*. [1991]. The ratio TEC/$N_{max}$ varies far less than either parameter, and it is called the equivalent slab thickness ($\tau$)—meaning the effective altitude span of an ionosphere with a given TEC value formed by a layer of constant electron density equal to $N_{max}$. The global average for the Earth's ionosphere (under daytime conditions) is $<\tau>$ ~ 250 km. A practical use of that fact is that under average conditions one parameter can be obtained from the other—with relevance to radio propagation needs. For example, prior to the availability of global TEC measurements using the constellation of GPS satellites, the vast network of ground-based ionosondes was used to generate TEC from average slab thickness values.

### 2.4. The Scientific Relevance of Slab Thickness

Under photochemical equilibrium conditions, the resultant ionosphere is highly dependent upon the neutral atmosphere that is ionized; and thus, $\tau$ values have long been considered a first-order indicator of the scale height ($H = kT_n/\mathrm{mg}$) of the background neutral atmosphere. This relationship was shown explicitly by *Wright* [1960]. When a $N_e(h)$ profile follows the functional pattern associated with so-called $\alpha$-Chapman theory, its integral results in $\mathrm{TEC} = 4.133 \times H \times N_{max}$, giving the useful approximation

$$\tau \sim 4 \times H \quad (4)$$

When applied to the terrestrial ionosphere (with atomic oxygen the dominant neutral at the height of $N_{max}$), the $<\tau> = 250$ km value results in $T_n = 1190$°K, a typical value of exospheric temperature under moderate solar flux conditions. *Titheridge* [1973] described a comprehensive use of $\tau$ values to infer the neutral exospheric temperature ($T_{exo}$) versus local time, season, and solar cycle.

### 2.5. Slab Thickness of the Martian Ionosphere

Given the use of $\tau$ values to estimate neutral temperatures at Earth prior to their direct measurement, can TEC and $N_{max}$ observations from MEX/MARSIS lead to slab thickness values that can serve as indicators of upper atmospheric temperatures? An initial assessment is immediately possible since a single slab thickness value, averaged overall solar fluxes and zenith angles, can be obtained by simply dividing equation (3) by equation (1); the resultant value is ~50 km. When inserted into $\tau = 4.133\,H$, and using **g** at Mars and $CO_2$ as

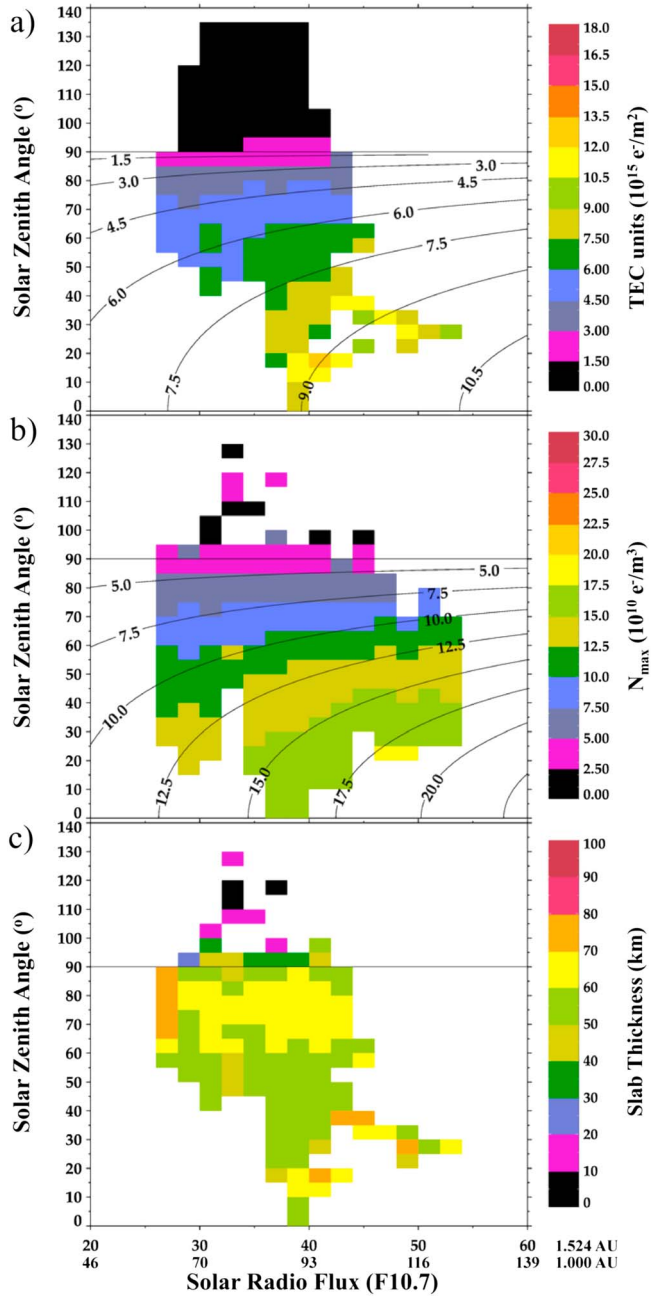


**Figure 1.** Results of TEC, $N_{max}$, and $\tau$ for the common data period of MEX/MARSIS AIS and SS-mode observations in 2005–2007. (a) Pattern of TEC versus SZA and solar radio flux. (b) Pattern of $N_{max}$ versus SZA and solar radio flux. The contours in Figures 1a and 1b give model values from equations (1) and (3), respectively. (c) Slab thickness versus SZA and solar radio for the common data bins in Figures 1a and 1b. The solar radio fluxes ($F_{10.7}$) at 1 AU were converted to values at 1.524 AU assuming a $1/d^2$ dependence for this standard proxy for EUV.

the dominant neutral for $h \leq 215$ km [*Krasnopolsky*, 2002], one obtains $T_n$(°K) $= 4.83 \times \tau$(km). Mindful that integer accuracy is all that is warranted by the simplifying assumptions made, we adopt

$$T_n(°\mathrm{K}) \sim 5 \times \tau(\mathrm{km}) = 250°\mathrm{K} \quad (5)$$

This is a reasonable daytime thermospheric temperature averaged over solar cycle conditions—as embodied in the use of equations (1) and (3).

## 3. Analysis of Common Data Sets

### 3.1. Diurnal Pattern

Encouraged by the above result from semiempirical models, we conducted a pure data analysis study of slab thickness values formed from compatible observations. The MARSIS/AIS and SS-mode observations of $N_{max}$ and TEC shared a common data period from 15 August 2005 to 30 September 2007. While this ~2 year observing period spans the same years, the overall data taking duty cycle is divided between the two MARSIS radar modes; and thus, each mode has its own data rate. Using both daytime and nighttime conditions, there were 687,250 high-quality TEC values and 31,885 $N_{max}$ values available for study. The observational uncertainty for TEC is ~0.35 TEC units for daytime (~6% of daytime mean) and 0.15 units (~50%) for nighttime [*Mouginot et al.*, 2008; *Mendillo et al.*, 2013a]. For $N_{max}$, the radio sounding measurement uncertainty was quoted to be about 2% [*Duru et al.*, 2008; *Mendillo et al.*, 2013b]. Somewhat higher values were suggested (10% daytime for TEC and 5% for $N_{max}$) by *Sanchez-Cano et al.* [2015]. Using these larger independent error estimates for daytime TEC and $N_{max}$, the resultant observational error for slab thickness would be ~11%—a factor of 2 below the variability patterns we present below.

We sorted the TEC and $N_{max}$ values into 2 × 2 bins in units of SZA and RF (adjusted for Mars' average distance at 1.524 AU and orbital location, as described in *Mendillo et al.* [2013a]). This gives a globally averaged perspective, i.e., no regional analyses for sectors with or without strong crustal magnetic fields were

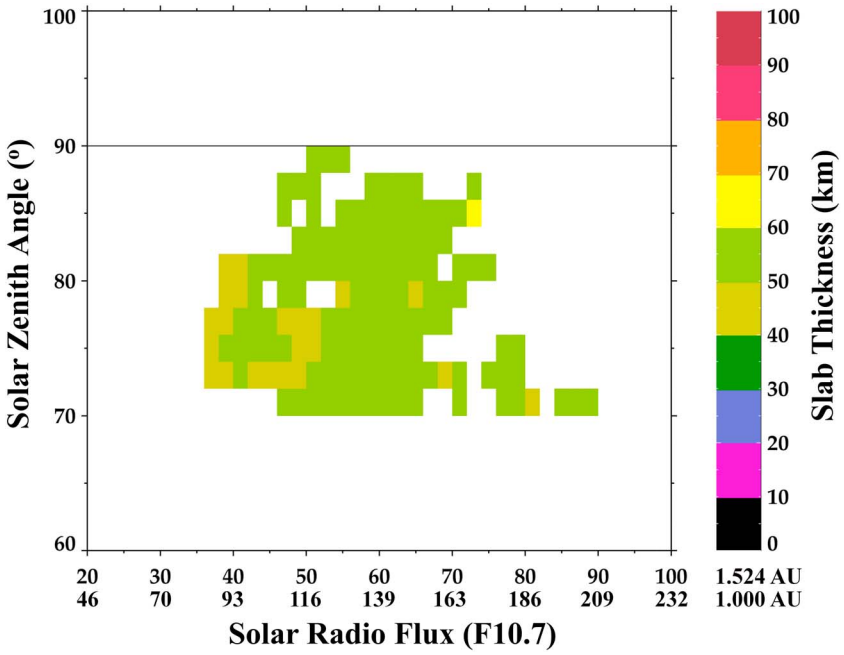


**Figure 2.** The pattern of slab thickness versus SZA and solar flux derived using values of TEC and $N_{max}$ from MGS $N_e(h)$ radio occultation profiles between 100 and 200 km near the dawn and dusk terminators.

attempted. The results appear in Figure 1a for TEC and Figure 1b for $N_{max}$. There are fewer nighttime values (SZA $>$ 90°) for $N_{max}$ in Figure 1, and the TEC values span a more limited range of solar fluxes than for $N_{max}$. The overall patterns for TEC and $N_{max}$ versus SZA and solar flux show the morphologies typical of an ionosphere in photochemical equilibrium (PCE). The contours resulting from equations (1) and (3), superposed on the data, can help describe the iso-value patterns. The equal value contours are nearly horizontal at high SZA values for all solar fluxes, showing that the ionosphere decays to essentially the same nighttime values regardless of solar cycle conditions. The equal value contours are more vertical at low SZA (midday conditions) when changing solar fluxes have their strongest effect.

Dividing Figure 1a by Figure 1b further restricts the results since $\tau$ values can only be formed from the bins containing both data sets, as shown in Figure 1c. Nevertheless, the resultant slab thickness results offer some preliminary conclusions. High $\tau$ values occur near midday (SZA $<$ 20°), with somewhat lower values in the SZA range 40°–60°. The highest $\tau$ values occur near-terminator conditions (70°–90°), with the lowest $\tau$ values at night (SZA $>$ 100°).

### 3.2. Solar Cycle Pattern

The MGS radio occultation profiles offer a significantly broad coverage of solar cycle conditions to enable a longer-term analysis of slab thickness patterns. Measurement error is a few $\times 10^3$ $e^-/cm^3$ [*Mendillo et al.*, 2004]—about an order of magnitude lower than electron densities over the 100–200 km height range that we use to form a consistent set of TEC values. The statistical variabilities (standard deviations of a monthly mean) for TEC and $N_{max}$ are both about 10% [*Mendillo et al.*, 2003, 2004]. For MGS $N_e(h)$ profiles, the TEC and $N_{max}$ values naturally refer to the same space and time. Yet all of the profiles have a limited SZA range of ~70°–90°. This does offer, however, the opportunity to compare results with the MARSIS solar minimum patterns for those high SZA conditions. Using MGS TEC values and their corresponding $N_{max}$ values, the resulting pattern of $\tau$ versus SZA and solar radio flux appears in Figure 2. In comparison to Figure 1c, the solar flux range is larger and the coverage at high SZA is, of course, excellent. The values of $\tau$ at low ($<$40 units) and high ($>$80 units) solar flux come from few data points, and thus represent the largest uncertainties.

### 3.3. Average Temperature Patterns

Given the small range of solar flux values (25–45 units at Mars) in Figure 1c, we decided to average over these solar minimum conditions to obtain the average pattern of $\tau$ and $T_n$ versus SZA. This is shown in Figure 3a,

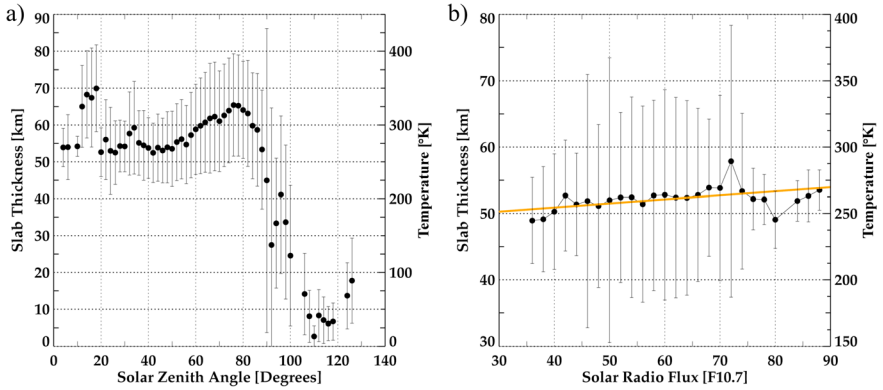


**Figure 3.** (a) The pattern of slab thickness and derived temperature versus solar zenith angle obtained by averaging the MARSIS $\tau$ values in Figure 1c over the solar flux conditions shown. The left axis gives $\tau$ values, and the right axis converts them to temperature values using equation (5). The average variability ($\sigma$) about the mean values is ±60°K (±25%), while the average error of the mean ($\sigma/\sqrt{n}$) is less than 1%. The $\tau$(km) and $T$(°K) values for SZA > 100° are not considered statistically reliable due to the division of two very low magnitude values that approach observational uncertainties. The high $\tau$ and $T$ values between 10° and 20° SZA appear inconsistent with the overall trend—probably due to limited coverage in those data bins (see Figure 1c). (b) The pattern of MGS slab thickness and derived temperature versus solar flux at Mars obtained by averaging the $\tau$ values in Figure 2 over the limited solar zenith angle range shown. The average variability ($\sigma$) about the mean values is ±55°K (±21%), while the average error of the mean ($\sigma/\sqrt{n}$) is ±5°K (±2%). The linear fit shown is dominated by midday conditions (SZA between 45° and 75°) and is given as equation (6).

with the slab thickness scale on the left and its corresponding neutral thermospheric temperature scale on the right. There are few data points available for very low solar zenith angles (SZA ≤ 20°)—conditions that might otherwise be of concern, as discussed in by *Sanchez-Cano et al.* [2015]. Similarly, few data points occur for very high SZAs (≥100°). Thus, the trend of interest is for SZAs in the range 20°–100°. The pattern that emerges is one of essentially constant midday temperatures, with somewhat higher values near the sunrise and sunset periods (SZA = 70°–90°). A dramatically cooler thermosphere is evident for the presunrise and postsunset times (SZA = 90°–100°). Given that the MEX orbit resulted in far more MARSIS observations in the dusk sector than near dawn (as shown for TEC in Figure 1 of *Mendillo et al.* [2013a]), the terminator trend is essentially for evening local times. Figure 3a thus offers the first attempt to relate ionospherically derived neutral temperatures to local time conditions during a period of low solar flux ($<F_{10.7}>$ = 35 units at Mars).

Just as we averaged over a small range of solar flux values to get Figure 3a, we now average over the small range of SZAs in Figure 2 to get Figure 3b. This represents the first attempt to use ionospheric observations to infer the solar cycle pattern for thermospheric temperatures. The data between 40 and 80 solar flux units are the most reliable, and they dominate the curve-fitting method used to obtain a functional relationship:

$$T_n(°\mathrm{K}) = 245°K + 0.25 \times F_{10.7} \quad (6)$$

where $F_{10.7}$ is the solar flux averaged over three solar rotations, and the Pearson correlation coefficient is 0.45.

The temperature patterns in Figures 3a (diurnal) and 3b (solar cycle) raise several questions of interpretation. First, we address variability versus error bars. The vertical bars in Figures 3a and 3b give variability ($1\sigma$) about the mean and thus do not represent errors. The large number of data points used (nearly 32,000 for Figure 3a and ~5000 for Figures 3b) yield "errors of the mean" ($\sigma/\sqrt{n}$) that are a fraction of a kilometer in Figures 3a and ~1 km in Figures 3b, and therefore <1°K and 5°K, respectively. The results thus portray meaningful global average conditions. More of a concern is the specification of the relevant height for the inferred temperature. Given that TEC is dominated by plasma near and above $h_{max}$, the $\tau$ values obtained (and therefore temperatures) should be appropriate for a height between $h_{max}$ (typically ~130 km) and a few scale heights (at ~12–15 km each) into the topside ionosphere. We adopt an average topside ionosphere height of 160 km—an altitude consistent with the typical median of contributions to the TEC integral between 80 and 400 km—as well as with PCE conditions breaking down at ~170 km. Models of temperature versus height [e.g., *Krasnopolsky*, 2002] show that the thermosphere at Mars does not achieve its final (exospheric) temperature ($T_{exo}$) at either $h_{max}$ or 160 km, but rather near 200 km for low solar

conditions ($F_{10.7} = 30$ at Mars), near 210 km for moderate solar activity ($F_{10.7} = 60$ at Mars), and ~240 km for solar maximum conditions ($F_{10.7} = 77$ at Mars). The temperature differences between 160 km and at these three heights of $T_{exo}$ also depend on the phase of the solar cycle. From Krasnopolsky's curves, this $\Delta T$ is ~10°K for solar minimum, ~30°K for solar moderate, and ~65°K for solar maximum. Using average solar flux conditions as an example, $T_{exo} \sim T_n + 30$°K, with $T_n$ given by equation (6). Our conclusion is that neutral atmosphere temperatures derived from slab thickness should be treated as thermospheric values and not as temperatures of the exosphere.

## 4. Discussion

### 4.1. Previous Estimates of Slab Thickness: Earth, Mars, and Saturn

While there are many past studies of slab thickness patterns found versus latitude, season, solar cycle, and geomagnetic storm conditions at Earth [*Titheridge*, 1973; *Fox et al*., 1991; *Mendillo et al*., 1972], there are only two previous studies of $\tau$ at other planets. For Mars, three early MGS data sets of $N_e(h)$ profiles during the years 1998–2000 were used to form TEC between 100 and 200 km. When divided by their $N_{max}$ values, the 209 profiles yielded $< \tau > = 53.3 \pm 6.1$ km [*Mendillo et al*., 2004]. This near-terminator value is essentially identical to the 52.8 km average from the full set of 5600 MGS profiles shown in Figures 2; and thus, the MGS results show a consistent long-term average relationship between TEC and $N_{max}$.

Radio occultation experiments have also been conducted in the outer solar system. The largest number to date comes from the Cassini radio science experiment at Saturn [*Kliore et al*., 2009]. *Moore et al*. [2010] analyzed a set of 37 profiles spanning solar flux conditions ranging from 66 to 116 units at Earth, with latitude coverage between ~ ±75°. The results obtained showed a remarkably consistent value for average slab thickness ($\tau_{saturn}$ ~1500 km) but with values consistently higher at dawn versus dusk. While *Moore et al*. [2010] did not relate their $\tau$ values to temperatures, a $< \tau >$ of ~1500 km leads to $T_{exo} \sim 900$ K when equation (4) is used with Saturn's scale height for a neutral atmosphere dominated by $H_2$. As shown in *Mueller-Wodarg et al*. [2006], this is about twice the accepted value for the exospheric temperature (~400 K) at Saturn. This raises an issue of possible relevance to Mars. For Saturn, the dominant ionospheric ions are $H_3^+$ and $H^+$ --- not the ionized version of the dominant neutral ($H_2$). At Mars, the dominant ions ($O_2^+$ and $O^+$) are also not the ionized versions of the dominant neutral ($CO_2$). Rapid chemistry converts the initially ionized species ($H_2^+$ at Saturn and $CO_2^+$ at Mars) to other ions that affect the vertical distribution of plasma at topside heights ($h > h_{max}$), where most of the TEC resides. This is not the case at Earth where the major ion ($O^+$) comes directly from the ionization of the dominant neutral (O) in the thermosphere. For very small ionic masses (as at Saturn), the low-mass species can have a dramatic influence upon slab thickness due to vertical plasma diffusion effects—enhancing the extent of the ionosphere and thus its TEC. Such effects would occur to a far less extent for heavy ionic masses (as at Mars). Modeling studies, beyond the scope of the present paper, are clearly needed to explore possible modifications to the first-order scaling factor we use (based on simple Chapman theory) between slab thickness, derived scale heights, and therefore neutral temperatures.

### 4.2. Martian Slab Thickness Considerations: Spatial Issues

A unique issue for slab thickness analyses is the height range over which TEC is calculated—and thus how consistent the numerator is in the definition $\tau = \text{TEC}/N_{max}$. For the Mars Express satellite carrying the MARSIS instrument, the peri-apse height is ~ 300 km (with apo-apse at ~10,000 km) and thus its radar signals traverse a broad range of altitudes to and from the surface. Yet the Martian ionosphere is rather limited in extent, with models showing that it merges with the dayside solar wind at heights usually below 400 km. Given that the vast majority of TEC values from MARSIS are from satellite heights above 400 km, we are confident in assuming that the observed TEC is the full TEC. However, for the Mars Global Surveyor electron density profiles used to compute TEC, only the height range 100–200 km can provide a consistent approximation to TEC. Our model studies of observed electron density profiles from both MGS and MEX radio occultation experiments [*Mendillo et al*., 2011] indicate that the TEC below 200 km is typically 70% of that found from $N_e(h)$ profiles spanning 80–400 km. This suggests that slab thickness values computed from MGS profiles underestimate $\tau$ by about 30%, and consequently yield lower estimates of temperature. To check on this, one can compare the $\tau$ values obtained using MARSIS data (Figure 3a) to those obtained

from MGS profiles (Figure 3b) at comparable SZA values (~77°) and solar flux values (35 units). The MARSIS $<\tau>\sim 63$ km gives $T = 315$°K, while the MGS $<\tau>\sim 51$ km gives $T = 255$°K, suggesting that the MGS-derived temperatures are indeed ~75–80% of the MEX-derived temperatures.

### 4.3. Martian Slab Thickness Considerations: Comparisons With Previous Results

Direct in situ neutral temperature ($T_n$) profiles characterizing the thermosphere of Mars have only been achieved by the two Viking descent probes [*Nier and McElroy*, 1977]. Supplementing these are several sources of information about $T_n$ inferred from different types of observations, as summarized by *Lichtenegger et al*. [2006] and shown in Table 1 in *Stiepen et al*. [2015]. These include derivations of scale heights (and therefore temperatures) from satellite drag, orbital decay, and optical (UV) emissions. Initial models for Martian thermal structure versus height and local time appear in *Bougher et al*. [1999]. Their Figure 6 showed that for $h = 160$ km, the nighttime minimum $T_n$ was ~150°K prior to dawn and the daytime maximum was ~260°K at 1600 LT, with strong gradients at sunrise and sunset. The slab thickness-derived temperature patterns in Figure 3a for SZAs between 0° and 100° are broadly consistent with these predictions. *Němec et al*. [2011] derived best fit scale heights for the Chapman formula applied to MARSIS topside sounder data and found H to increase from 12.5 km to 18 km over the 0–80° SZA range. This corresponds to our trend in Figure 3a, but with equivalent slab thickness and temperature values higher than found in our combined analysis MARSIS TEC and $N_{max}$.

For the solar cycle pattern shown in Figure 3b, the satellite drag study of *Forbes et al*. [2006] is of direct relevance. They used a single year (2003) of MGS orbital drag results to derive the sensitivity of neutral temperature ($\Delta T$) at 390 km to changes in solar flux ($\Delta F$). The overall climatology (with $F_{10.7}$ ranging from 50 to 70 units at Mars) was described by $\Delta T/\Delta F = 0.47$. This doubles our equation (6) result of 0.25 over the $F_{10.7}$ range of 40 to 80 units shown in Figure 3b. However, when examined for periods with pronounced solar rotating (27 day) active regions, *Forbes et al*. [2006] found the sensitivity factor ($\Delta T/\Delta F$) to be a factor of 2 larger (0.78 to 1.15). A follow-up study using MGS drag over the years 1999–2005 found an even larger long-term sensitivity trend with $\Delta T/\Delta F$ ~1.5 [*Forbes et al*., 2008].

*Bougher et al*. [2009] used general circulation models to assess the *Forbes et al*. [2008] results and concluded that "tuning" the solar heating rates within accepted limits could reproduce the reported sensitivity factor. The range of $<F_{10.7}>_{81\ day}$ values used in *Forbes et al*. [2008] study was 40–110 units at Mars. This is somewhat larger than the statistically reliable portion of our Figure 3b where $F_{10.7}$ changed from 45 to 75 units. In addition, all of the MGS data in Figure 3b refer to near-terminator values when ionospheric patterns change most rapidly [*Fox and Yeager*, 2006]—rather than to the more stable daytime conditions described by *Forbes et al*. [2008]. With new TEC and $N_{max}$ data sets now available for daytime conditions from MARSIS (2007–2014) and TEC from the SHAllow RADar (2006–2013) on the Mars Reconnaissance Orbiter [*Campbell et al*., 2014], a more comprehensive set of slab thickness studies can be conducted for SZA and solar flux conditions.

The *Stiepen et al*. [2015] study of the Martian thermosphere used derived scale heights of ultraviolet day-glow observations from the emission profiles of CO Cameron bands (170–270 nm) and $CO_2^+$ emissions (298 nm and 299 nm) measured by the Spectroscopy for Investigation of Characteristics of the Atmosphere of Mars instrument on Mars Express [*Bertaux et al*., 2006]. Their data spanned the years 2003–2013, providing a range of solar flux conditions ($F_{10.7}$ at Mars of 25–55 units) and solar zenith angles (~20°–55°). Their scale heights of ultraviolet emissions ($H_{uv}$) were derived from limb scans of the Martian atmosphere between 150 and 180 km, with a mean height of 165 km. This is close to our assumed height of 160 km for the ionospheric slab thickness derivations of neutral scale height ($H_n$). The *Stiepen et al*. [2015] scale heights for both the CO and $CO_2^+$ emissions were mostly in the range 14–16 km (their Figures 7 and 8), in excellent agreement with our MARSIS derived daytime average value of $<\tau>\sim 60$ km ($H_n = 15$ km) in Figure 1c.

The *Stiepen et al*. [2015] results for correlation of $H_{uv}$ with solar zenith angles did not show a clear pattern over the range SZA = 20°–55°. Our analysis in Figure 3a, over a broader range of SZAs, is consistent with theirs—showing variability during daytime hours masking any underlying smooth local time pattern. Most interesting is their lack of correlation of daytime $H_{uv}$ with solar activity in the $F_{10.7}$ range 25–55 units at Mars. Our results—restricted to the dawn/dusk terminator conditions observed by MGS—span a larger range of solar activity and show a mild positive correlation with solar cycle changes. *Stiepen et al*. [2015]

concluded that their scale heights did not show significant correlations with latitude, season, local time, and solar flux because persistent atmospheric variability masks such patterns. Optical emission mechanisms are very sensitive to small changes in composition and density driven by a multitude of atmospheric dynamical processes, and thus the UV technique is best suited to documenting variability and broad morphologies, rather than specific SZA and $F_{10.7}$ effects.

## 5. Summary and Conclusions

We have conducted the first systematic study of independent data sets for the TEC and $N_{max}$ of the Martian ionosphere. The ratio TEC/$N_{max}$ yielded equivalent slab thickness ($\tau$) patterns versus SZA and solar flux. When $\tau$ results were converted to scale heights and temperatures, using the assumption of photochemical equilibrium (PCE), a broad consistency emerged with the few available measurements and models for thermospheric temperatures at Mars. Concerns about the height range over which TEC should be used within the context of PCE theory, and the availability of new data sets from Mars Atmosphere and Volatile Evolution (MAVEN), MEX and Mars Reconnaissance Orbiter, suggest that follow-up studies might better explore direct empirical relationships between $\tau$, scale height, and temperature.

**Acknowledgments**

At Boston University, this work was supported, in part, by the NASA MAVEN Mission grant NNX-13AO20G, the comparative aeronomy component of NSF grant AGS-1123222, the Undergraduate Research Opportunities Program (UROP), and seed research funds made available through the Center for Space Physics. The MARSIS data were made available, thanks to G. Picardi (Universita di Roma' La Sapienza', Rome, Italy), R. Orosei, and J. Plaut, as well as the European Space Agency. The data sets can be found at the ESA Planetary Science Archive. Data set MARS EXPRESS/MARSIS can be found in this website: ftp://psa.esac.esa.int/pub/mirror/MARS-EXPRESS/MARSIS. The MGS data are available at the PDS Geosciences node, website: http://pds-geosciences.wustl.edu/missions/mgs/rsdata.html.

The Editor thanks Arnaud Stiepen and an anonymous reviewer for their assistance in evaluating this paper.

## References

Bertaux, J.-L., et al. (2006), SPICAM on Mars Express: Observing modes and overview of UV spectrometer data and scientific results, *J. Geophys. Res.*, *111*, E10S90, doi:10.1029/2006JE002690.

Bougher, S., S. Engel, R. Roble, and B. Foster (1999), Comparative terrestrial planet thermospheres 2. Solar cycle variation of global structure and winds at equinox, *J. Geophys. Res.*, *104*, 16,591–16,611, doi:10.1029/1998JE001019.

Bougher, S., T. McDunn, K. Zoldak, and J. Forbes (2009), Solar cycle variability of Mars dayside exospheric temperatures: Model evaluation of underlying thermal balances, *Geophys. Res. Lett.*, *36*, L05201, doi:10.1029/2008GL036376.

Campbell, B., N. Putzig, F. Foss, and R. Phillips (2014), SHARAD signal attenuation and delay offsets due to the Martian ionosphere, *IEEE Geosci. Remote Sens. Lett.*, *11*(3), 632–635, doi:10.1109/LGRS.2013.2273396.

Cartacci, M., E. Amata, A. Cicchetti, R. Noschese, S. Giuppi, B. Langlais, A. Frigeri, R. Orosei, and G. Picardi (2013), Mars ionosphere total electron content analysis from MARSIS subsurface data, *Icarus*, *223*, 423–437, doi:10.1016/j.icarus.2012.12.011.

Duru, F., D. A. Gurnett, D. D. Morgan, R. Modolo, A. F. Nagy, and D. Najib (2008), Electron densities in the upper ionosphere of Mars from the excitation of electron plasma oscillations, *J. Geophys. Res.*, *113*, A07302, doi:10.1029/2008JA013073.

Forbes, J., S. Bruinsma, and F. Lemoine (2006), Solar rotation effects in the thermosphere of Mars and Earth, *Science*, *312*, 1366–1368.

Forbes, J., F. Lemoine, S. Bruinsma, M. Smith, and X. Zhang (2008), Solar flux variability of Mars' exosphere densities and temperatures, *Geophys. Res. Lett.*, *35*, L01201, doi:10.1029/2007GL031904.

Fox, J., and K. Yeager (2006), Morphology of the near-terminator Martian ionosphere: A comparison of models and data, *J. Geophys. Res.*, *111*, A10309, doi:10.1029/JA011697.

Fox, M., M. Mendillo, and J. Klobuchar (1991), Ionospheric equivalent slab thickness and its modeling applications, *Radio Sci.*, *26*, 429–438, doi:10.1029/90RS02624.

Gurnett, D., et al. (2005), Radar sounding of the ionosphere of Mars, *Science*, *310*, 1929–1933, doi:10.1126/science.1121868.

Hinson, D. P., R. A. Simpson, J. D. Twicken, G. L. Tyler, and F. M. Flasar (1999), Initial results from radio occultation measurements with Mars Global Surveyor, *J. Geophys. Res.*, *104*(E11), 26,997–27,012, doi:10.1029/1999JE001069.

Kliore, A., A. Nagy, E. Marouf, A. Anabtawi, E. Barbinis, D. Fleishchman, and D. Kahan (2009), Midlatitude and high-latitude electron density profiles in the ionosphere of Saturn obtained by Cassini radio occultation observations, *J. Geophys. Res.*, *114*, A04315, doi:10.1029/2008JA013900.

Krasnopolsky, V. (2002), Mars' upper atmosphere and ionosphere at low, medium and high solar activities: Implications for evolution of water, *J. Geophys. Res.*, *107*(A9), 1245, doi:10.1029/2001JE001809.

Lichtenegger, H., H. Lammer, Y. Kulikov, S. Kazeminejad, G. Molina-Cuberos, R. Rodrigo, B. Kazeminejad, and G. Kirchengast (2006), Effects of low energetic neutral atoms on Martian and Venusian dayside exospheric temperature estimations, *Space Sci. Rev.*, *126*, 469–501.

Lillis, R., D. Brain, S. England, P. Withers, M. Fillingim, and A. Safaeinili (2010), Total electron content in the Mars ionosphere: Temporal studies and dependence on solar EUV flux, *J. Geophys. Res.*, *115*, A11314, doi:10.1029/2010JA015698.

Mendillo, M., M. Papagiannis, and J. Klobuchar (1972), Average behavior of the mid-latitude *F* region parameters $N_T$, $N_{MAX}$ and $\tau$ during geomagnetic storms, *J. Geophys. Res.*, *77*, 4891–4895, doi:10.1029/JA077i025p04891.

Mendillo, M., S. Smith, J. Wroten, and H. Rishbeth (2003), Simultaneous ionospheric variability on Earth and Mars, *J. Geophys. Res.*, *108*(A12), 1432, doi:10.1029/JA00996.

Mendillo, M., X.-Q. Pi, S. Smith, C. Martinis, J. Wilson, and D. Hinson (2004), Ionospheric effects upon a satellite navigation system at Mars, *Radio Sci.*, *39*, RS2028, doi:10.1029/2003RS002933.

Mendillo, M., A. Lollo, P. Withers, M. Matta, M. Patzold, and S. Tellmann (2011), Modeling Mars' ionosphere with constraints from same-day observations by Mars Global Surveyor and Mars Express, *J. Geophys. Res.*, *116*, A11303, doi:10.1029/2011JA016865.

Mendillo, M., C. Narvaez, P. Withers, M. Matta, W. Kofman, and J. Mounigot (2013a), Variability in ionospheric total electron content at Mars, *Planet. Space Sci.*, *86*, 117–129, doi:10.1016/j.pss.2013.08.010.

Mendillo, M., A. Marusiak, P. Withers, D. Morgan, and D. Gurnett (2013b), A new semi-empirical model of the peak electron density of the Martian ionosphere, *Geophys. Res. Lett.*, *40*, 5361–5365, doi:10.1002/2013GL057631.

Moore, L., I. Mueller-Wodarg, M. Galand, A. Kliore, and M. Mendillo (2010), Latitudinal variations in Saturn's ionosphere: Cassini measurements and model comparisons, *J. Geophys. Res.*, *115*, A11317, doi:10.1029/2010JA015692.

Mouginot, J., W. Kofman, A. Safaeinili, and A. Herique (2008), Correction of the ionospheric distortion on the MARSIS surface sounding echoes, *Planet. Space Sci.*, *56*, 917–926, doi:10.1016/j.pss.2008.01.010.

Mueller-Wodarg, I. C. F., M. Mendillo, R. V. Yelle, and A. D. Aylward (2006), A global circulation model of Saturn's thermosphere, *Icarus*, *180*, 147–160.

Němec, F., D. Morgan, D. Gurnett, F. Duru, and V. Truhlik (2011), Dayside ionosphere of Mars: Empirical model based on data from the MARSIS instrument, *J. Geophys. Res.*, *116*, E07003, doi:10.1029/2010JE003789.

Nier, A., and M. McElroy (1977), Composition and structure of Mars' upper atmosphere—Results from the neutral mass spectrometers on Viking 1 and 2, *J. Geophys. Res.*, *82*, 4341–4349, doi:10.1029/JS082i028p04341.

Pätzold, M., S. Tellmann, B. Häusler, D. Hinson, R. Schaa, and G. Tyler (2005), A sporadic third layer in the ionosphere of Mars, *Science*, *310*, 837–839, doi:10.1126/science.1117755.

Picardi, G., et al. (2005), Radar soundings of the subsurface of Mars, *Science*, *310*(5756), 1925–1928, doi:10.1126/science.1122165.

Safaeinili, A., W. Kofman, J. Mouginot, Y. Gim, A. Herique, A. Ivanov, J. Plaut, and G. Picardi (2007), Estimation of the total electron content of the Martian ionosphere using radar sounder surface echoes, *Geophys. Res. Lett.*, *34*, L23204, doi:10.1029/2007GL032154.

Sanchez-Cano, B., et al. (2015), Total electron content in the Martian atmosphere: A critical assessment of the Mars Express MARSIS datasets, *J. Geophys. Res. Space Physics*, *119*, doi:10.1002/2014JA020630.

Stiepen, A., J.-C. Gerard, S. Bougher, F. Montmessin, B. Hubert, and J.-L. Bertaux (2015), Mars thermospheric scale height: CO Cameron and $CO_2$+ dayglow observations from Mars Express, *Icarus*, *245*, 295–305.

Titheridge, J. E. (1973), The slab thickness of the mid-latitude ionosphere, *Planet. Space Sci.*, *21*, 1775–1793.

Wright, J. (1960), A model of the *F* region above $h_mF_2$, *J. Geophys. Res.*, *65*(1), 185–191, doi:10.1029/JZ065i001p00185.